

Calibration of Thermal Models of Continuous Casting of Steel

Lance C. Hibbeler¹, Melody M. Langeneckert¹, Junya Iwasaki¹, Inwho Hwang¹, Ron J. O'Malley², Brian G. Thomas¹

1 - The University of Illinois at Urbana-Champaign
Department of Mechanical Science and Engineering
1206 West Green Street
Urbana, Illinois, 61801, USA
Tel.: +1-217-333-6919

E-mail: lhibbel2@illinois.edu, hwang104@illinois.edu, bgthomas@illinois.edu

2 - Nucor Steel Decatur
4301 Iverson Boulevard
Trinity, Alabama, 35673, USA
Tel.: +1-256-301-3524
E-mail: ron.omalley@nucor.com

Key words: Model Calibration, Mold Heat Transfer, Continuous Casting, Computational Model

ABSTRACT

Computational models of continuous casting can reveal a great deal about the process, as long as they are able to match the real caster. A simple one-dimensional model of heat conduction in the mold is accurate except near the thermocouples, bolt holes, and cooling-water channel roots where the details of the three-dimensional geometry affects the mold heat transfer. To overcome this obstacle, which is important during model calibration, a new methodology is presented to calibrate the one-dimensional CON1D model with a full three-dimensional finite-element model of the mold. Specifically, the thermocouple depth in the 1-D model CON1D is "offset" to account for both the 3-D geometric effects and for the heat removed along the thermocouple wire by water or air convection. With the offset, this simple 1-D model can match closely with the 3-D model. The fast CON1D model then is easily calibrated to match plant heat-flux and thermocouple measurements. Coupled with models of solidification and interfacial phenomena, this accurate and efficient modeling tool is easily applied to gain insights into many aspects of heat transfer in the process.

INTRODUCTION

The harsh environment of commercial steel continuous casting processes makes measurements difficult, expensive, and limited in the information gained. Computational models potentially offer deeper knowledge, but only if they can accurately predict the plant behavior. This requires including and solving the equations which govern all of the important physical phenomena. To achieve reasonable speed while retaining accuracy, computational models must be simplified and calibrated to match plant experiments, using parameters which remain constant over the range of processing conditions of interest. Only after verification, calibration, and validation, can a model be used reliably as a predictive tool to investigate complex processes such as continuous casting.

Development of an accurate computational model requires verification, calibration, and validation. Verification refers to matching the model predictions exactly with the known analytical solution of a simple well-defined test problem, in order to prove error-free programming of the chosen numerical methods, and to find reasonable choices for mesh and time-step discretizations. Validation refers to matching the model predictions with plant experiments, to ensure that the equations being solved contain the appropriate physics, and that the properties and constants in those equations have good values. Calibration is usually needed to find values for those constants to match the plant measurements and achieve validation. These last two activities generally require multiple iterations. This paper illustrates this activity for the computational model of heat transfer in continuous casting of steel, CON1D¹.

The CON1D model has been successfully applied to many commercial casters in previous work^{2,3,4,5,6}, and is described in detail elsewhere¹. This paper focusses on the calibration procedure to improve its accuracy. The procedure first involves a full three-dimensional computation of the mold, to produce average results for a “calibration domain”. Input parameters to the CON1D model are defined and calibrated to match the average hot face and thermocouple temperatures from the 3D model. Then, CON1D can be calibrated to match thermocouple measurements and heat flux measurements taken from plant operation. Finally the model can be applied to gain new insights into the process.

THREE-DIMENSIONAL MODEL OF MOLD: CALIBRATION DOMAIN

The steady-state temperature distribution in the continuous-casting mold is determined by solving the steady heat-conduction equation for temperature as a function of the three coordinate directions $T(x, y, z)$:

$$\frac{\partial}{\partial x} \left(k \frac{\partial T}{\partial x} \right) + \frac{\partial}{\partial y} \left(k \frac{\partial T}{\partial y} \right) + \frac{\partial}{\partial z} \left(k \frac{\partial T}{\partial z} \right) = 0 \quad (1)$$

where k is the isotropic thermal conductivity. The temperature dependence of the thermal conductivity of mold copper alloys of about $-0.05 \text{ \%}/^\circ\text{C}$ ⁷ has only a small effect on the typical mold temperature field.⁷ This effect is readily included, but the governing equation for the calibration procedure is simplified here for constant conductivity:

$$\frac{\partial^2 T}{\partial x^2} + \frac{\partial^2 T}{\partial y^2} + \frac{\partial^2 T}{\partial z^2} = 0 \quad (2)$$

Boundary conditions include specified heat flux at the mold hotface:

$$-k_0 \frac{\partial T}{\partial n} = q_0 \quad (3)$$

where k_0 is the average thermal conductivity, q_0 is the heat load that may vary with position and $\partial T / \partial n$ is the temperature gradient normal to the mold surface. On the water channels, a constant convection condition is specified:

$$-k_0 \frac{\partial T}{\partial n} = h_0 (T - T_0) \quad (4)$$

by defining the heat transfer coefficient h_0 and “sink” temperature T_0 .

The finite element method is used to solve these equations in the complicated-shaped domain of the modern casting mold, owing to its accurate handling of arbitrary geometries. This work uses the commercial finite-element software ABAQUS⁹, combined with scripts written in Python code to automate creation of the geometry, running of the analysis, and post processing the results to extract the parameters needed for the one-dimensional CON1D model, as discussed later. The aim of this model is to enable the simple 1D model of the mold, CON1D, to achieve the accuracy of a complete three-dimensional analysis of the multi-dimensional heat flow around the roots of water channels and thermocouple holes.

The 3D model domain should reproduce the exact geometry of an appropriate periodic or symmetric portion of the mold geometry. The 3D model results can be used directly to reveal local heat transfer variations within this fundamental domain, such as hot face temperature variations around the mold perimeter between bolts. For the calibration of the 1D model, the 3D model results are spatially-averaged over this symmetrically-repeating domain, to extract the average hot face temperature $T_{hot,3D}$, the average cold face temperature $T_{cold,3D}$, and the average temperature on the small surface that contacts the thermocouple $T_{TC,3D}$. These 3 temperatures are needed for the 1D model calibration. In addition, the 3D model results reveal insights into important mold temperature variations. Modern computer platforms can solve this problem, even with very fine mesh resolution, with execution times on the order of a few minutes.

ONE-DIMENSIONAL MODEL OF MOLD

To model heat transfer in continuous casting requires accurate incorporation of the mold, interface, and solidifying shell. Away from the corners, many phenomena can be modeled reasonably well with a one-dimensional assumption. The CON1D model is based on a one-dimensional finite-difference solidification model of the shell, taking advantage of the large Péclet number that makes axial heat conduction negligible relative to heat transported by the moving steel. It includes conduction and radiation across the interfacial layers, aided by mass, momentum, and force balances on the slag, which are all solved analytically. For efficiency, heat conduction through the mold is modeled analytically. Axial heat conduction in the mold, which is important near the meniscus, is handled with a

two-dimensional series solution^{1,2,4}. Through the thickness direction, the coated copper plate is treated as a series of one-dimensional thermal resistances. The water slot region is treated as a convection surface in parallel with heat-conduction fins. Further details are given below.

The mold in the CON1D model is envisioned as a rectangular block with rectangular water channels, as shown in Figure 1. All water channels are identical with depth d_c , width w_c , and pitch p_c . The hot side of the mold is supplied a heat flux q_{hot} from the interface and solidification models, described elsewhere¹. Heat is extracted from the water channel surfaces via a convection condition $h_{cold}(T_{cold} - T_{water})$. The temperature distribution inside the mold is found by integrating directly Equation (1) and applying these two boundary conditions:

$$T(x) = T_{water} + q_{hot} \left(\frac{1}{h_{cold}} + \frac{d_{mold} - x}{k_{mold}} \right) \quad (5)$$

where x is the distance away from the hot face and d_{mold} is the simulated mold thickness. Coating layers are included by adding $d_{coating}/k_{coating}$ resistors inside the parentheses¹. This gives a cold face temperature of $T_{cold} = T(L) = T_{water} + q_{hot}/h_{cold}$ and a hot face temperature of $T_{hot} = T(0) = T_{water} + q_{hot}(1/h_{cold} + d_{mold}/h_{cold})$. The cold side heat transfer coefficient is adjusted to include scale deposits as another thermal resistance:

$$\frac{1}{h_{cold}} = \frac{d_{scale}}{k_{scale}} + \frac{1}{h_w} \quad (6)$$

where d_{scale} and k_{scale} are the thickness and thermal conductivity of any scale layers on the channel sides, and h_w is the fin-enhanced heat transfer coefficient of the nominal water convection coefficient h_{water} :

$$h_w = h_{water} \frac{w_c}{p_c} + \frac{1}{p_c} \sqrt{2(p_c - w_c)h_{water}k_{mold}} \tanh \left(d_c \sqrt{\frac{2}{(p_c - w_c)k_{mold}} h_{water}} \right) \quad (7)$$

The first term accounts for the heat leaving the roots of the channels, while the second term accounts for the heat transferred through the lateral surfaces of the fins. This equation assumes a large number of rectangular channels that are very long in the casting direction, and that heat loss into the backing plate or waterbox is negligible. Of many empirical correlations for the water convection coefficient, the forced-internal-flow correlation of Sleicher and Rouse¹⁰ is chosen for its accurate fit with many measurements (about 7% average error):

$$Nu = 5 + 0.015 Re^a Pr^b \quad (8)$$

The Nusselt number $Nu = h_{water} D_h / k_{water}$, Prandtl number $Pr = \mu_{water} c_{p,water} / k_{water}$, and Reynolds number $Re = \rho_{water} V_{water} D_h / \mu_{water}$ respectively are evaluated at the temperature of the bulk water T_{water} , the temperature of the channel surface T_{cold} , and the ‘‘film’’ temperature $T_{film} = \frac{1}{2}(T_{water} + T_{cold})$. The hydraulic diameter, defined as four times the cross-sectional area divided by the perimeter, is $D_h = 2w_c d_c / (w_c + d_c)$ for a rectangular channel, and $a = 0.88 - 0.24/(4 + Pr)$ and $b = 1/3 + 0.5 \exp(-0.6 Pr)$ are fitting constants. The water velocity V_{water} is found from the total water flow rate in the plant and the total water-channel area. The water properties⁴ vary with temperature ($^{\circ}C$) as follows:

$$k_{water}(T) = 0.59 + 0.001 \cdot T \quad (9)$$

$$\mu_{water}(T) = 2.062 \cdot 10^{-9} \rho_{water} \cdot 10^{792.42/(T+273.15)} \quad (10)$$

$$\rho_{water}(T) = 1000.3 - 0.040286 \cdot T - 0.0039779 \cdot T^2 \quad (11)$$

$$c_{p,water}(T) = 4215.0 - 1.5594 \cdot T + 0.015234 \cdot T^2 \quad (12)$$

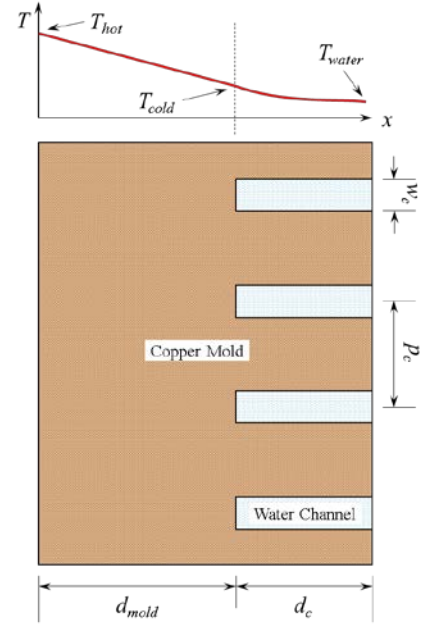


Figure 1. One-Dimensional Mold Model

Measurements available at most casters include thermocouple temperatures and the average heat flux, based on the mold water flow rate and its temperature increase. In the one-dimensional CON1D model approximation, thermocouple temperatures T_{TC} are obtained by evaluating Equation (5) at the appropriate distance beneath the hot face d_{TC} :

$$T_{TC} = T_{water} + q_{hot} \left(\frac{1}{h_{cold}} + \frac{L - d_{TC}}{k_{mold}} \right) \quad (13)$$

The increase in temperature of the mold water as it flows through the channels is found by applying a heat balance on a differential slice through the water and integrating over the working mold length:

$$\Delta T_{water}(z) = \frac{p_c}{w_c d_c} \frac{1}{V_{water}} \int_0^z \frac{q_{hot}(z')}{\rho_{water}(z') c_{p,water}(z')} dz' \quad (14)$$

where V_c is the casting speed and $t = z/V_c$ is the time corresponding to distance z below meniscus. This assumes that all heat entering the mold is removed by the mold water. This prediction of mold temperature rise must be modified to account for unused water channels when casting narrow slabs relative to the mold width and, if applicable, the fact that the water channels might not all have the same dimensions and pitch:

$$\Delta T'_{water} = \Delta T_{water} \frac{w_{slab}}{p_c} \frac{w_c d_c}{A_{channels}} \quad (15)$$

where w_{slab} is the slab width and $A_{channels}$ is the total cross-sectional area of the channels. After geometric calibration described in the next section, a second calibration / verification stage should be performed to ensure that this prediction of the water temperature rise matches with the plant measurements.

ONE-DIMENSIONAL MODEL CALIBRATION

Simplifying the mold geometry for the one-dimensional model requires careful definition of the dimensions in order to retain the thermal characteristics of the system. The geometric parameters in the 1D model described above are the simulated mold thickness L , the channel width w_c , the channel depth d_c , and the channel pitch p_c . By choosing these parameters carefully, the one-dimensional model can attain the predictive capability of the 3D finite-element calculation mentioned previously. This section presents the equations to accomplish this, which have been implemented into the Python script and are executed after postprocessing of the finite-element results, prior to running CON1D.

Water Channel Geometry

The water channels in the 1D model must have identical cross-sectional area to the physical mold to maintain the mass flow rate of the cooling water. To maintain the convection coefficient in the water channels, the hydraulic diameter must be the same as well. For a single channel, this requires:

$$w_c d_c = A_{c,actual} \quad (16a)$$

$$2w_c d_c / (w_c + d_c) = D_{h,actual} \quad (16b)$$

where $A_{c,actual}$ and $D_{h,actual}$ are the actual cross-sectional area and hydraulic diameter of the channel. These two equations are solved simultaneously to give:

$$w_c, d_c = A_{c,actual} / D_{h,actual} \pm \sqrt{\left(A_{c,actual} / D_{h,actual} \right)^2 - A_{c,actual}} \quad (17)$$

where the smaller of the two roots is the channel width and the larger root is the channel depth. Note that both roots are positive because $A_{c,actual}$ and $D_{h,actual}$ are positive. If the mold has different types of channels, which is common around bolt holes, then the actual channel area and hydraulic diameter should be their respective averages for all N channels across the width of the repeating portion of the mold, modeled in the 3D calculation:

$$A_{c,actual} = \frac{1}{N} \sum_{i=1}^N A_{c,actual,i} \quad (18a)$$

$$D_{h,actual} = \frac{1}{N} \sum_{i=1}^N D_{h,actual,i} \quad (18b)$$

Note that Equation (17) is not applicable if all channels are round. An approximation that relaxes Equation (16b) is used for this case⁶. Specifically, setting $w_c = 0.7 D$ produces an error in the convection coefficient of only 2%.

The simulated channel pitch should be chosen to minimize the variations caused by different channel sizes. Consider the cumulative channel cross-sectional area plotted with distance along a symmetric portion of the mold width, schematically illustrated in Figure 2. The one-dimensional model approximates this cumulative area as a straight line with a slope that defines the simulated channel pitch p_c :

$$A_{cumulative,simulated}(x) = \frac{A_{c,actual}}{p_c} x \quad (19)$$

The details of the actual cumulative area function are specific to an individual mold, but a simple least-squares fit is sufficient to determine a good simulated pitch.

Next, the simulated mold thickness d_{mold} should be chosen such that the hot face temperature matches the 3D simulation under identical boundary conditions. Evaluating Equation (5) at the hot face, matching the result to the average hot face temperature calculated with the 3D model, and rearranging, gives:

$$d_{mold} = \frac{k_0}{q_0} (T_{hot,3D} - T_{w0}) - \frac{k_0}{h_{cold}} \quad (20)$$

Since $h_{cold} \gg k_{mold}$, the second term of Equation (20) usually is negligible. To match the 3D calculation, the temperature-dependency of the properties and the scale layer are neglected during calibration, so Equations (6) and (7) simplify to:

$$h_{cold} = h_0 \frac{w_c}{p_c} + \frac{1}{p_c} \sqrt{2(p_c - w_c) h_0 k_0} \tanh \left(d_c \sqrt{\frac{2}{(p_c - w_c) k_0}} \frac{h_0}{k_0} \right) \quad (21)$$

Note that for some geometries, this calibration method causes the parameter d_{mold} to be significantly larger than the distance between the hot face and water channel roots, d_{cold} . The distance from the hot face to where the cold face temperature is found in the 1D model is defined as:

$$d'_{mold} = d_{mold} - \frac{k_0}{q_0} (T_{cold,3D} - T_{w0}) = \frac{k_0}{q_0} (T_{hot,3D} - T_{cold,3D}) \quad (22)$$

Depending on the choice of $T_{cold,3D}$, the cold face temperature predicted by CON1D can be chosen to match the root, average, or other desired definition of cold face temperature. Defining the cold face temperature as the average root temperature over all channels gives d'_{cold} close to the physical distance between the hot face and water channels.

This calibration method enables the 1D model to match the hot-face and cold-face temperatures calculated in the 3D model, by changing the water channel input geometry in a physically-based manner.

Thermocouple Hole Geometry

The thermocouple temperature predicted by the CON1D model may differ from the temperature predicted by the 3D finite-element model at the same location^{6,11}. Depending on the geometry, this error has been observed to exceed 50 °C. This mismatch is due to the inability of the 1D model to capture the effects of complicated geometry near the thermocouple bore. However, this problem can be overcome by changing the location of the simulated thermocouple. By moving the thermocouple point in the 1D model closer to the hot face, the 1D model can reliably reproduce the hotter thermocouple temperature predicted by the three-dimensional model, regardless of heat flux, mold material, and water channel behavior.

By manipulating Equation (13), the simulated thermocouple depth in the calibrated 1D model should be:

$$d'_{TC} = d_{mold} - \frac{k_0}{q_0} (T_{TC,3D} - T_{w0}) = \frac{k_0}{q_0} (T_{hot,3D} - T_{TC,3D}) \quad (23)$$

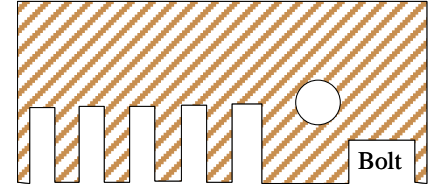
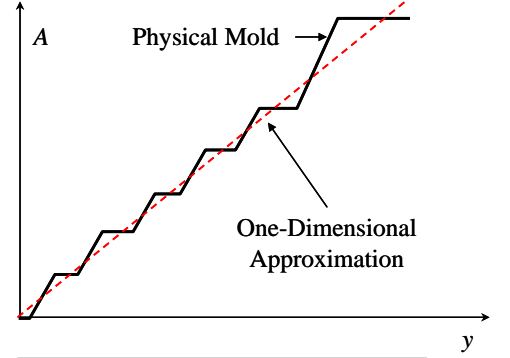


Figure 2. Simulated Channel Pitch Should Match Cumulative Channel Area

This calibration of the thermocouple location should be performed after the water channel geometry has been calibrated using Equations (17), (19), and (21). Even though the terms appear in Equation (23), d'_{TC} is independent of heat flux, conductivity, and mold geometry. This observation is demonstrated later.

Offset Methodology

In the interest of a user-friendly model interface, it is convenient to express each calibrated dimension as the “blueprint” value and an “offset” distance. This approach also shows how important were the calibrations. For example, the mold thickness offset distance Δd_{cold} is defined as:

$$\Delta d_{cold} = d'_{cold} - d_{cold} \quad (24)$$

and the thermocouple offset distance Δd_{TC} is:

$$\Delta d_{TC} = d'_{TC} - d_{TC} \quad (25)$$

Because calibration is independent of heat load and mold properties, the offset calculation needs to be performed only once for a given mold geometry.

Thermocouple Wire Heat Removal

Measured thermocouple temperatures often read low due to contact resistance between the thermocouple bead and the cold face where the thermocouple is touching. Heat is lost by conduction along the length of the thermocouple wires, especially if they are long and well-cooled. Assuming that the thermocouples behave as long circular rod-fins, they extract heat with rate:

$$q_{TC} = \sqrt{\frac{4}{D} h k_{TC}} (T_{TC} - T_0) \quad (26)$$

where D is the thermocouple diameter, k_{TC} is the conductivity of the thermocouple, h is the heat transfer coefficient along the thermocouple wire to the surrounding medium at temperature T_0 , and T_{TC} is the thermocouple temperature. The heat transfer coefficient should be around 5 kW/m²·K for water or 0.1 kW/m²·K for air.

The thermocouple temperature T'_{TC} accounting for this heat loss can be modeled using another heat-conduction resistor:

$$T'_{TC} = T_{TC} + \frac{d_{gap}}{k_{gap}} q_{TC} \quad (27)$$

where T_{TC} is the predicted thermocouple temperature which, for the 1D model, is from Equation (13), using the calibrated thermocouple depth d'_{TC} from Equation (22), and d_{gap} and k_{gap} are the size and thermal conductivity of the gap between the thermocouple and the mold copper. The gap conductivity should be about 1.25 W/m·K for a thermal paste or about 0.04 W/m·K for dry still air. The gap size is typically on the order of 0.01 to 0.1 mm, but can be treated as a calibration parameter to force the models to match plant measurements. This approach of calibrating thermocouple temperatures has been demonstrated in recent works presented elsewhere^{12,13}.

EXAMPLE CALIBRATIONS

The calibration procedure presented in this work is demonstrated for two commercial casting molds with complicated mold geometries. Both are uncoated thin-slab mold wide faces, one with and one without a funnel. Four cases, summarized in Table 1, are considered to prove the method for different geometries and processing conditions.

Mold A is 1986 mm wide, 950 mm long, and 40 mm thick. It has a rectangular array of mold bolts at 108 mm in the width direction and 133 mm in the casting direction, except for the top and bottom row of bolts. There are three rows of thermocouples at 205, 355, and 505 mm below the top of the mold, spaced at 108 mm in the width direction, directly in between bolt columns. The calibration domain models a typical thermocouple in the middle row of thermocouples, extending to its four nearest bolts. The periodic nature of this mold geometry allows use of the “fundamental” calibration domain shown in Figures 3-5. As seen in Figure 3, the water channels immediately adjacent to the bolt columns curve around the bolt holes; except for these regions, the channel pitch is 17.7 mm. Each fundamental domain has six 16-mm deep ball-end-milled channels, which run almost the entire length of the mold between any two

adjacent columns of bolt holes. The two channels directly adjacent to a column of bolt holes are 6 mm wide, while the “standard” channels are 5 mm wide.

Mold B is 1860 mm wide, 1100 mm long, and 80 mm thick. It has a funnel that is 750 mm wide with a 260-mm wide “inner flat” region. The funnel tapers from a 23.4-mm crown to an 8-mm crown at mold exit. This mold has a rectangular array of mold bolts at 212.5 mm in the width direction and 125 mm in the casting direction. There is a thermocouple hole drilled into every bolt hole, except for the topmost row and outermost columns of bolts. The water channels consist of banks of 18 ball-end milled channels, 5-mm across, 15-mm deep, and 10-mm pitch, between two bolt columns, with gun-drilled 12-mm circular channels immediately adjacent to the bolt holes. The calibration domain models a typical thermocouple outside of the funnel region, and includes one circular channel and nine ball-end-milled channels.

3D Model Results

The 3D model of the mold contains the exact geometry of a portion of the mold geometry, chosen here as the fundamental domain shown in Fig. 3, for Case 1. The three process parameters input to this model are simply:

- ◆ the mold conductivity k_0
- ◆ a uniform heat flux to the hot face q_0
- ◆ a uniform water channel convection coefficient h_0 and water temperature T_{w0}

The finite element model predicts hot face temperatures ranging from 243.8 to 251.1 °C with an average hot face temperature $T_{hot,3D} = 248$ °C, average cold face temperature $T_{cold,3D} = 96.6$ °C, (taken at the water channel roots), and thermocouple temperature $T_{TC,3D} = 146$ °C. The calculated temperature contours for Case 1 are shown in Figures 3-5. These results show that the highest hot face temperature in this mold geometry, found opposite the bolt nearest to the thermocouple, is about 7 °C hotter than the minimum temperature around the mold perimeter. It is not known if this hotface temperature variation is significant for longitudinal crack formation.

Table 1. Simulation Parameters and Results

	Case 1		Case 2		Case 3		Case 4	
	A 3D	A 1D	A 3D	A 1D	B 3D	B 1D	B 3D	B 1D
Mold								
Thermal Conductivity k_0 (W/m·K)		340		326		350		300
Heat Flux q_0 (MW/m ²)		2.10		2.35		3.00		2.71
Water HTC h_0 (kW/m ² ·K)		32.5		29.0		40.0		27.0
Water Temperature T_{w0} (°C)		31.0		30.0		35.0		37.0
Hot Face Temperature T_{hot} (°C)	248	248.1	286	287.1	312	310.4	339	340.3
Mold Thickness L (mm)		35.1		35.5		32.3		33.4
Cold Face Temperature T_{cold} (°C)	96.6	96.6	107	106.8	97.4	97.2	114.3	115.5
Distance to Cold Face d_{cold} (mm)	24	24.6	24	24.9	25	25.0	25	24.9
Cold Face Offset Δd_{cold} (mm)		-0.61		-0.90		-0.04		0.13
Thermocouple Temperature T_{TC} (°C)	146.0	146.3	167.0	168.3	159.7	159.8	180.3	181.5
Distance to Thermocouple d_{TC} (mm)	18	16.51	18	16.51	20	17.77	20	17.57
Thermocouple Offset Δd_{TC} (mm)		1.49		1.49		2.23		2.43

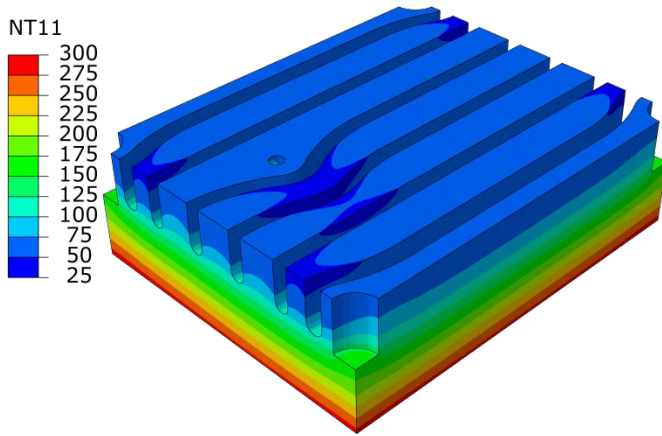


Figure 3. Mold Temperatures (°C) in Mold Calibration Domain from 3D Model (Case 1)

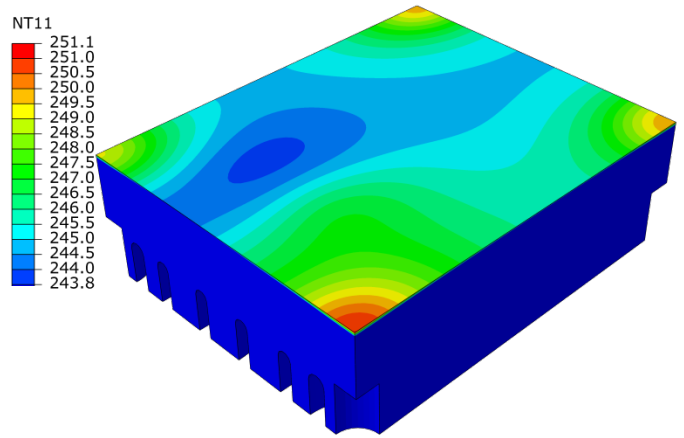


Figure 4. Hot Face Temperatures (°C) in Mold Calibration Domain from 3D Model (Case 1)

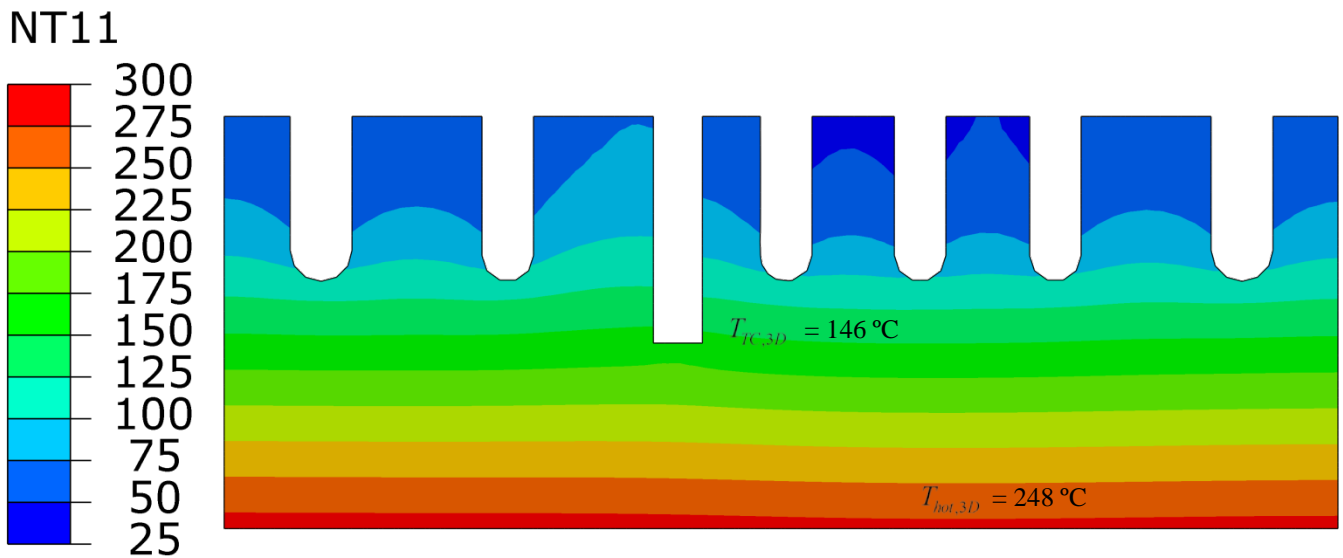


Figure 5. Mold Temperatures (°C) from 3D Model Near Thermocouple (Case 1)

Geometric Calibration of CON1D with 3D Model

Equation (17) gives the calibrated channel width and depth as 5.647 mm and 14.566 mm respectively. Figure 6 shows the determination of the channel pitch as 18.05 mm (average channel area of 82.26 mm² divided by the least squares slope of 4.556 mm²/mm). Using Equation (21), the effective heat transfer coefficient is then 37.65 kW/m²-K, so Equation (20) gives the calibrated mold thickness as 35.12 mm. Using identical boundary conditions and these calibrated geometries in CON1D gives a hot face temperature of 248.1 °C, which matches well with the 3D model. Using a thermocouple depth of 16.52 mm as calculated by Equation (23) instead of the nominal 18 mm (offset of 1.48 mm), the CON1D thermocouple temperature is 146.27 °C, which again matches well with the 3D model. Using a cold face depth of 24.61 mm instead of the nominal 24 mm (offset of 0.61 mm), the CON1D prediction exactly matches the 3D model cold-face temperature of 96.6 °C.

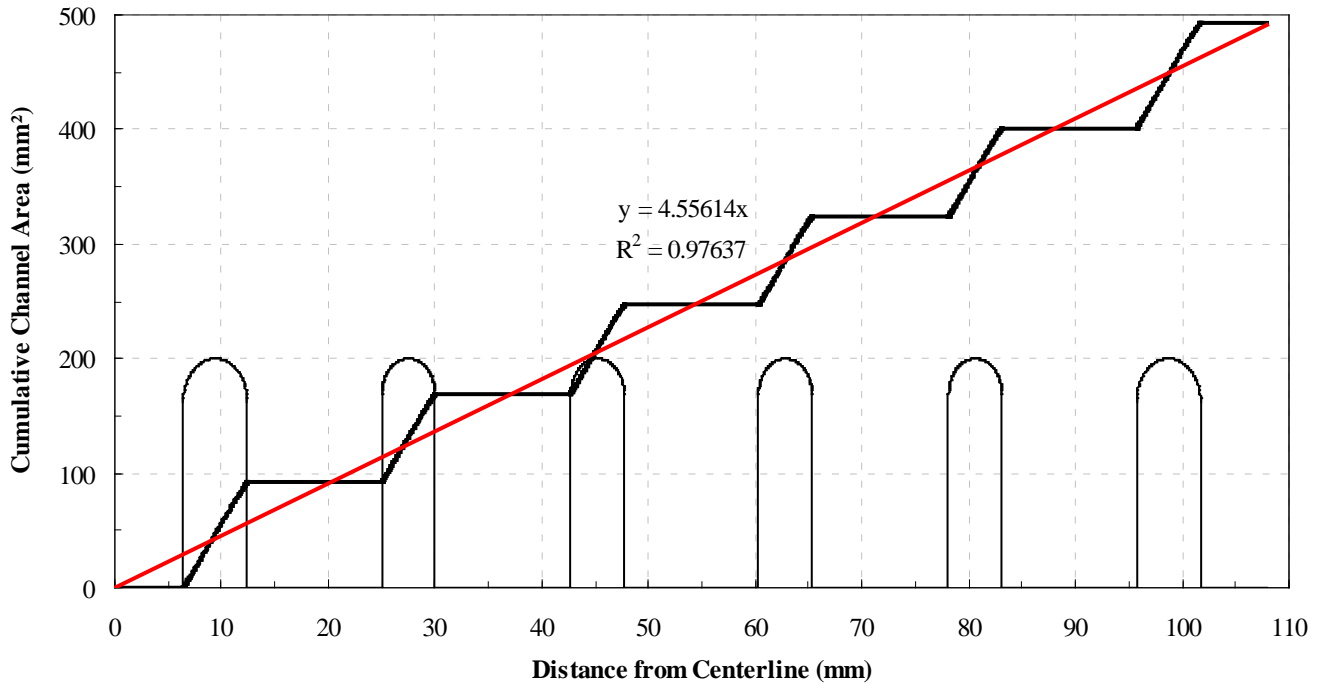


Figure 6. Determination of the One-Dimensional Channel Pitch

Table 1 shows the results of implementing this calibration procedure for different geometries and different processing parameters. Repeating the calibration procedure after changing the boundary conditions and thermal conductivity for mold A (Case 2) gives very similar calibrated geometries. For mold B, the calibrated channel is 5.84 mm wide and 13.07 mm deep, with a pitch of 10.63 mm. Again, repeating the calibration procedure with different thermal loading conditions and material properties, produces nearly-identical calibrated distances for the same mold geometry. The thermocouple offsets of 2.23 and 2.43 mm reported here are nearly the same as the 2.41 mm offset that was calculated in previous work⁶. More careful calculation of the average temperatures would likely produce calibrated distances that are even more similar. Nevertheless, the calibration procedure outlined here is independent of boundary conditions, and only needs to be performed once per mold geometry.

Heat Transfer Calibration of CON1D with Plant Data

Once the mold geometry has been properly calibrated, the mold water heat removal predicted by CON1D should be calibrated to match plant measurements. Previous work⁶ details this process for a wide variety of conditions for mold B. For example, consider casting a 0.045 %C steel at 4.5 m/min: the plant measures 2.55 MW/m² and CON1D calculates 2.54 MW/m² after calibration. Figure 7 shows that the CON1D predictions of thermocouple temperatures, once calibrated for geometric effects, match well with the maximum of the plant measurements at all thermocouples. The thermocouple calibration procedure was performed only once in this case, assuming perfect contact ($d_{gap} = 0$), and was applied to all thermocouples in the simulated mold. Intermittent nonzero contact resistance is believed to explain why some of the plant thermocouples give lower temperatures.

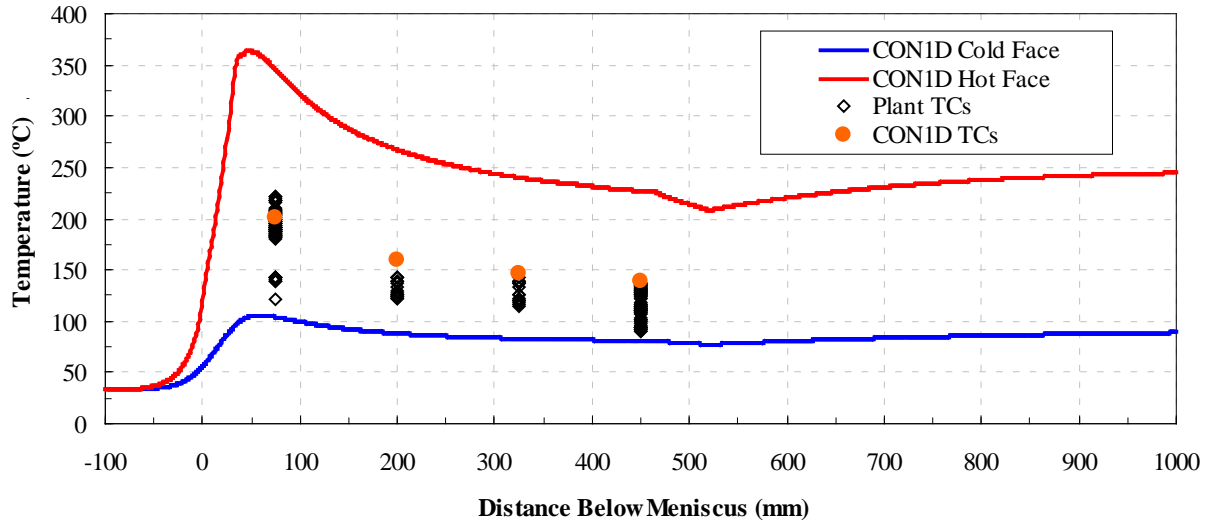


Figure 7. Calibrated CON1D Matches Plant Thermocouple Measurements

EXAMPLE APPLICATION: EFFECT OF MOLD WEAR ON SCALE FORMATION

After it has been calibrated both geometrically with the 3D model and thermally with plant measurements, as described in the previous section, the accurate 1D model is ready to apply to investigate a variety of heat transfer phenomena. As a simple example application, the CON1D model that was calibrated and validated in this work for Mold A was applied to study the formation of scale as the mold wears. Scale is assumed to form when the water in the channels is first able to boil, which is assumed to be a possibility when the surface temperature of the root of the channel – the calibrated cold face temperature – exceeds the boiling temperature. The boiling temperature in °C depends on the pressure as follows¹⁴:

$$T_{boil} = \frac{1810.94}{8.14019 - \log_{10}(7500.62 \cdot p)} - 244.485 \quad (28)$$

where p is the local pressure in the cooling channels in MPa. As the distance to the channels decreases with mold wear, the mold hotface temperature decreases, but the coldface temperature increases, for a given heat flux. Using Equation (28) with the CON1D results, we can identify the critical peak heat flux into the mold at which boiling and scale deposits could form. At the example operation pressure of 1.1 MPa, the critical coldface temperature is 184.3 °C, and the critical local heat flux drops from 5.15 to 3.68 MW/m² with just 4 mm of mold wear. Scale layers serve to increase mold temperature: specifically, CON1D predicts that a 5- μ m-thick scale layer will increase both hotface and coldface surface temperatures by more than 20 °C. Some worn molds have been observed to operate with higher average heat removal, and the smaller resistance to heat flow from the thinner mold is insufficient to explain this⁶. The application here suggests that scale formation associated with the mold wear could be a possible explanation. Scale formation problems can be minimized by maintaining high-purity water quality, keeping high water velocity, and careful design of water channels and water delivery system to avoid pressure drops. Note also that thinner molds tend to have lower temperatures, which helps to prevent scale formation with a lower cold face temperature. However, since the heat transfer from the shell into the mold depends on the interfacial gap resistance associated more with hot face temperature, the net effect on overall heat transfer depends on the mold flux behavior⁶. The results here suggest that molds should be paired as matching sets, wear should be regularly monitored, and water channels should be carefully inspected for scale formation.

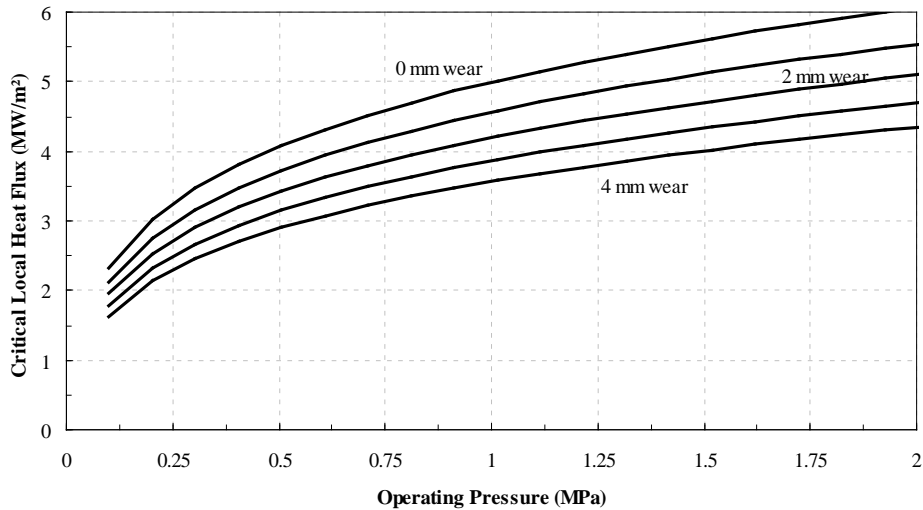


Figure 8. Critical Heat Flux for Scale Formation Decreases as Mold Wear Increases

CONCLUSIONS

This work has derived and demonstrated a method for imparting the accuracy of a three-dimensional mathematical model of mold heat transfer into a one-dimensional model of the continuous casting process. Specifically, the water channel geometries and thermocouple position are changed slightly from their respective “blueprint” values to compensate for multi-dimensional heat transfer. The calibration procedure was demonstrated to be independent of process conditions, so needs to be performed only once per mold geometry. Once this geometric calibration is performed, the shell-mold interfacial parameters in the fast one-dimensional model can be calibrated to match plant data, and then the model can be applied to accurately investigate various aspects of heat transfer in the continuous casting process.

An example application is provided to show that a scale layer is more likely to form for older, thinner molds. The three-dimensional models used in this work show the variation of mold surface temperature due to the geometric features of the mold. Future work is needed to quantify the allowable variability in mold surface temperature to avoid defects in the cast steel.

ACKNOWLEDGMENTS

The authors gratefully acknowledge the financial support of the member companies of the Continuous Casting Consortium at the University of Illinois at Urbana-Champaign, and the National Science Foundation (Grant CMMI 09-00138 REU).

REFERENCES

1. Y. Meng and B.G. Thomas, “Heat Transfer and Solidification Model of Continuous Slab Casting: CON1D.” *Metallurgical and Materials Transactions*, Vol. 34B, No. 5, 2003, pp. 685-705.
2. M.R. Ridolfi, B.G. Thomas, G. Li, U. Della Foglia, “The Optimization of Mold Taper for the Ilva-Dalmine Round Bloom Caster.” *La Revue de Metallurgie - CIT*, Vol. 91, No. 2, 1994, pp. 609-620.
3. J. Sengupta, M.K. Trinh, D. Currey, and B.G. Thomas, “Utilization of CON1D at ArcelorMittal Dofasco’s No. 2 Continuous Caster for Crater End Determination.” *Proceedings of AISTech 2009*.
4. G. Li, B.G. Thomas, B. Ho, G. Li, and N. Youssef, “CON1D User Manual,” CCC Report, University of Illinois, July, 1992.
5. Y. Meng and B.G. Thomas, “Simulation of Microstructure and Behavior of Interfacial Mold Slag Layers in Continuous Casting of Steel.” *ISIJ International*, Vol. 46, No. 5, 2006, pp. 660-669.
6. B. Santillana, L.C. Hibbeler, B.G. Thomas, A. Hamoen, A. Kamperman, and W. van der Knoop, “Heat Transfer in Funnel-mould Casting: Effect of Plate Thickness.” *ISIJ International*, Vol. 48, No. 10, 2008, pp. 1380-1388.
7. I.V. Samarasekera and J.K. Brimacombe, “The Thermal Field in Continuous-Casting Moulds.” *Canadian Metallurgical Quarterly*, Vol. 18, No. 3, 1979, pp. 251-266.
8. S. Chenna Krishna, N. Supriya, Abhay K. Jha, Bhanu Pant, S. C. Sharma, and Koshy M. George, “Thermal Conductivity of Cu-Cr-Zr-Ti Alloy in the Temperature Range of 300–873 K,” *ISRN Metallurgy*, Vol. 2012, Article ID 580659, 4 pages, 2012.
9. ABAQUS 6.11 User Manuals, 2011. Dassault Simulia, Inc., 166 Valley Street, Providence, RI, USA 02909.
10. C.A. Sleicher and M.W. Rouse, “A Convenient Correlation for Heat Transfer to Constant and Variable Property Fluids in Turbulent Pipe Flow.” *International Journal of Heat and Mass Transfer*, Vol. 18, No. 5, 1975, pp. 677-683.

11. M.M. Langeneckert, "Influence of Mold Geometry on Heat Transfer, Thermocouple and Mold Temperatures in the Continuous Casting of Steel Slabs." MS Thesis, The University of Illinois at Urbana-Champaign, 2001.
12. L.C. Hibbeler, S. Koric, K. Xu, B.G. Thomas, and C. Spangler, "Thermo-Mechanical Modeling of Beam Blank Casting." *Iron and Steel Technology*, Vol. 6, No. 7, 2009, pp. 60-73.
13. L.C. Hibbeler, B.G. Thomas, R.C. Schimmel, and G. Abbel, "Thermal Distortion of Funnel Molds", *Proceedings of AISTech 2011*.
14. NIST Webbook. <http://webbook.nist.gov>.

APPENDIX

To calculate the cumulative channel area, the following equation defines the area of a semicircle of diameter d as a function of distance along the diametrical edge, for $0 \leq x \leq d$:

$$A(x) = \frac{d^2}{4} \left[\frac{1}{2} \arccos \left(1 - 2 \frac{x}{d} \right) - \left(1 - 2 \frac{x}{d} \right) \sqrt{\frac{x}{d} \left(1 - \frac{x}{d} \right)} \right] \quad (29)$$